SAYARIM INFRASOUND CALIBRATION EXPLOSION: NEAR-SOURCE AND LOCAL OBSERVATIONS AND YIELD ESTIMATION

Yefim Gitterman

Geophysical Institute of Israel

Sponsored by the Army Space and Missile Defense Command

Award No. W9113M-07-C-0189
Proposal No. BAA07-52

ABSTRACT

A large-scale calibration explosion of about 82 tons of high explosives (HE), assembled as a pyramid on a soft sediment surface, was successfully conducted by the Geophysical Institute of Israel (GII) at Sayarim Military Range (SMR), Negev Desert, Israel, on 26 August 2009.

Near-source high-pressure values, measured in the range 200–600 m, were higher than predicted, whereas the resulting crater and the seismic magnitude were smaller than expected for this on-surface charge. These results confirm that the explosives, charge design, and upward detonation generated the necessary explosion energy and partition: a maximum of energy to the atmosphere and a minimum to the ground.

The high-pressure observations were utilized for reliable estimation of the important ground truth parameter—TNT equivalent yield of about 0.1 kt, based on a stable integral characteristic of air-blast waves—the positive phase impulse. As with near-source pressure gauges, anomalous enhanced peak pressure amplitudes were found at local infrasound stations, indicating possible an upward directivity effect and asymmetric energy radiation to the atmosphere.

Clear infrasound signals were well observed at distances up to 3,500 km at numerous portable and permanent stations in Israel, Mediterranean countries, and north-central Europe, including two International Monitoring System (IMS) stations I26DE and I48TN, which provided for this region the first full GT0 source dataset for on-surface, large-scale explosions recorded by infrasound stations of IMS.

Additional estimations of the explosion yield, based on empirical scaling relations for the peak amplitude, dominant period, and crater dimensions, were analyzed. Yield estimations from far-regional IMS infrasound stations, obtained at the International Data Centre (IDC) using trial published empirical yield-range-amplitude attenuation laws, were significantly overestimated, thus indicating the need for refinement and tuning of the monitoring procedures.

Observations jointly obtained with GT0 source parameters provided an extensive dataset for analysis and modeling of long-range atmospheric propagation of infrasound signals, detection, source location, and yield estimation.

OBJECTIVES

1) To conduct a surface explosion of 80 tons, providing the first large-scale GT0 infrasound source for Middle East/Mediterranean/Europe region for calibration of IMS and national infrasound stations and improvement of monitoring capabilities
2) To develop a charge design, providing maximum explosion energy to the atmosphere
3) To provide an extensive infrasound dataset from stations deployed at a broad of distances (0.1–3000 km)
4) To provide a reliable yield estimation of the explosion based on near-source observations and compare that estimation with estimations from local and far-regional distances

RESEARCH ACCOMPLISHED

Activities and research during the project's second year included final preparations for conducting the main surface calibration explosion at Sayarim and observing infrasound waves in a broad distance range. Obtained data and records were used to analyze empirical scaling relations for the peak amplitude, dominant period, and crater dimensions and to evaluate the TNT equivalent yield.

Testing the Feasibility of New Explosives and Charge Design

New HE explosives supplied by IMI Ltd. were used as the charge main agent for the Sayarim Calibration Explosion. The explosives were composed of recuperated TNT and some other HE components. Laboratory testing by IMI showed an average detonation velocity of ~7500 m/s, much higher than for standard TNT (6800 m/s). The cast explosives were supplied in big cardboard barrels (each one 315 kg). The last test was conducted several days before the main explosion (Table 1) to estimate energy release in the charge units (barrels) and transfer of the upward detonation through layers of charge. Two barrels were assembled as a tower on a wooden platform (Figure 1). The booster (mine M15, 10 kg of Composition B) was placed upside down (to provide an additional upward cumulative effect) beneath the platform. Two Bikini mechanical gauges were used for characterizing near-source high pressures.

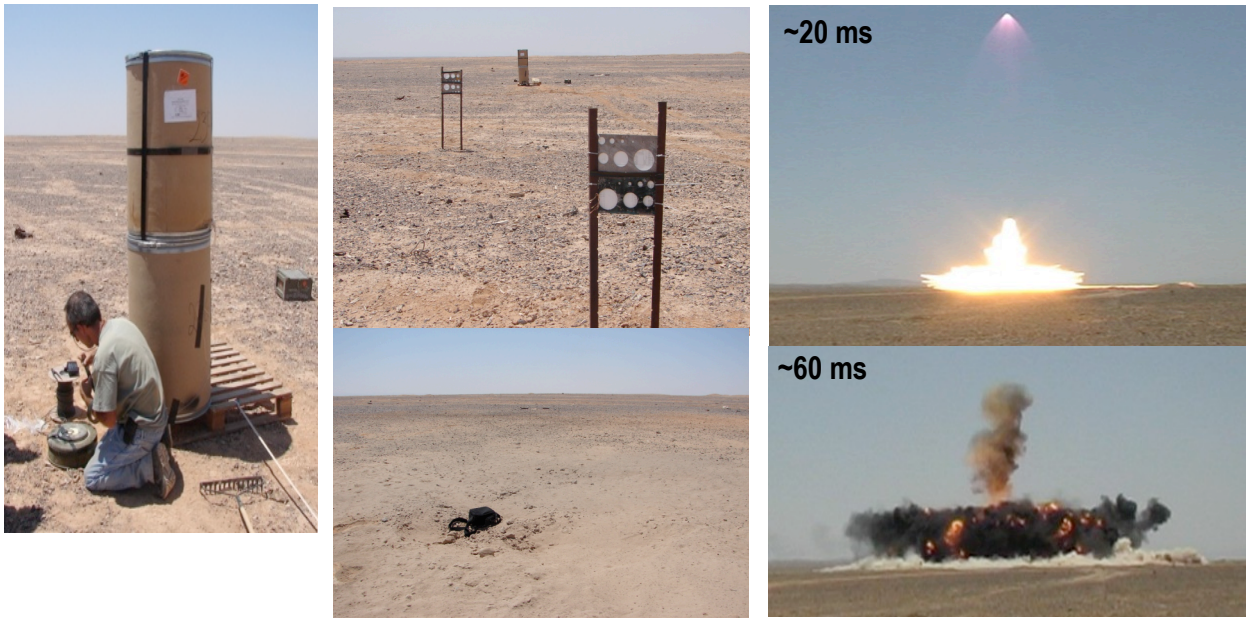

Figure 1. Preparation of the test shot charge of 640 kg (left) and observations: two Bikini gauges with two sets of holes glued by paper membranes and the explosion crater with a camera bag for scale (center); and snapshots from a home video recording, with the time after the detonation shown (right).

The gauges showed higher pressures than predicted for the equal TNT charge, and a very small crater was created. Both these features were evidence of a high efficiency for the selected explosives, charge design, and upward detonation conception, resulting in enhanced energy radiation to the atmosphere and low coupling to the ground.

Table 1. Parameters of explosions, conducted at Sayarim Military Range (SMR), Negev Desert, Israel

Explosion	Date	Detonation Time, GMT	Altitude, m	Latitude	Longitude
Test 640 kg	18/08/09	10:10:40.16*	563	29.99522N	34.80792E
Main shot	26/08/09	06:31:54.00	556	30.00057N	34.81351E

* Estimated by the Israel Seismic Network (ISN)

Main Charge Design.

Major design conceptions, elaborated by GII, were maximal concentration of explosives in the charge to provide release of maximal energy to the atmosphere. Figure 2 shows the following features of the charge design: big barrels filled up to the top with strong, cast HE explosives (315 kg); minimal air voids between the barrels (accomplished by filling the voids with plastic bags of HE bulk explosives); minimal air voids between six charge layers (accomplished by removing wooden platforms, except for those under the first layer); approximately hemispherical (pyramidal), compact shape (actual measured dimensions: base 5.8 × 5.9 m, height 5.5 m); strong booster with 52 M15 mines on the ground, upside down to provide the upward detonation, and 63 mines on the central platform in the first layer; and a multiple (22-point) initiation scheme.

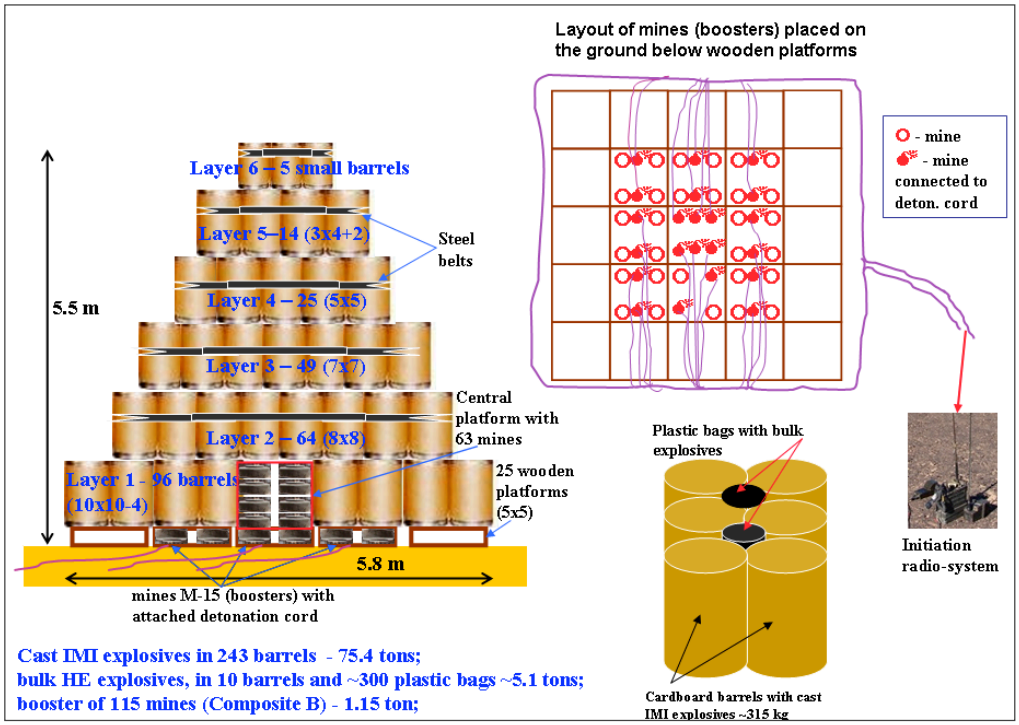

Figure 2. Charge shape and booster configuration and 22-point initiation design scheme.

The main charge was composed mostly of new, cast HE explosives by IMI, bulk HE explosives of different types, and Composition B in M15 mines, with the total nominal explosives weight of 81,664 kg. After the charge units on the platforms were specially prepared (in about 3 days), the charge was assembled during 1.5 days. The details of charge assembling and configuration are important for understanding the observed explosion effects and energy generation.

Conducting the Explosion and Near-Source Observations

The explosion was detonated on August 26, 2009, at ~9:30 AM local time. The day and time were chosen due to favorable wind conditions for infrasound propagation (Garces et al., 2009; Bowman et al., 2009). No wind was

observed during the explosion, evidenced by the vertical column of dust and gases (Figure 3). Accurately measured Greenwich Mean Time (GMT) for the detonation and GPS coordinates are presented in Table 1. Different measuring and observation systems were deployed at close distances: pressure gauges, accelerometers, and video cameras. The explosion layout and the locations of the systems are shown on Figure 3.

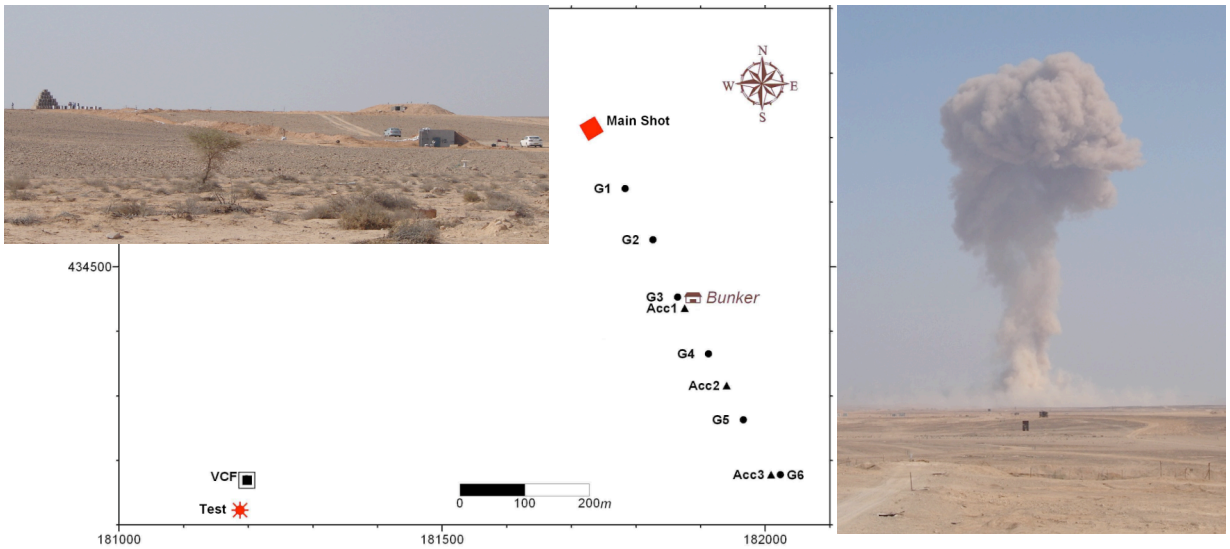

Figure 3. Explosion site view and layout, showing locations of the shots, the pressure gauges (G1–G6), accelerometers (Acc1–Acc3), and the speed video camera VCF (left); vertical light column of dust and gases of ~2 km height observed from the Command Post 5.8 km from the test and ~3 min after the detonation (right).

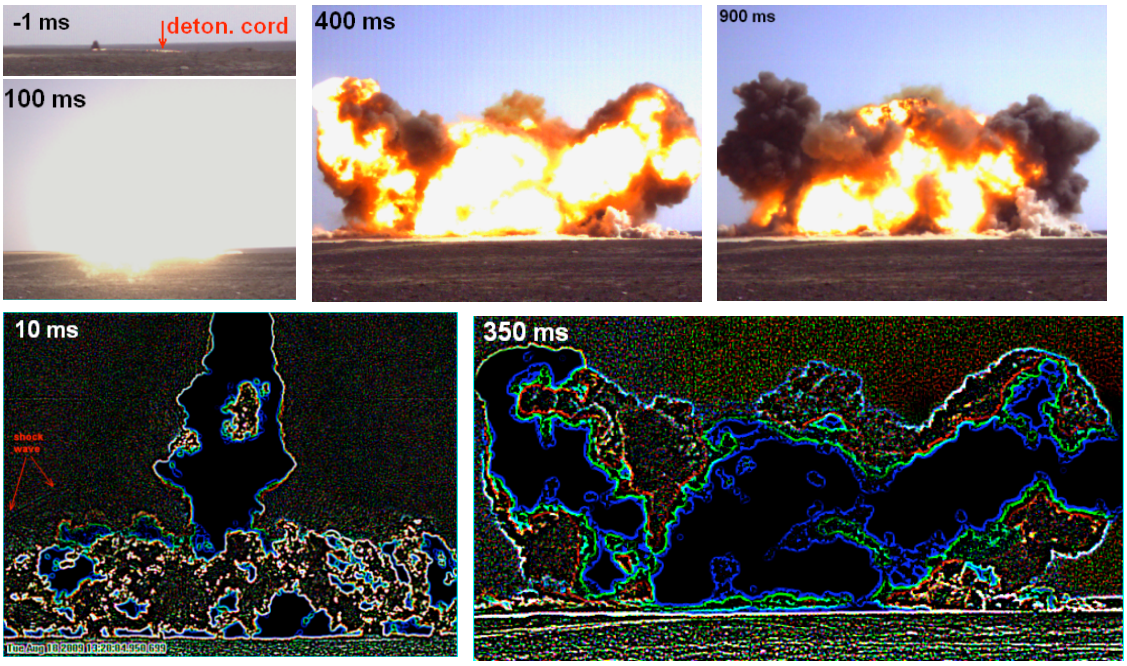

Figure 4. Sample snapshots from a speed video recording during the first second of the detonation (top). The explosion view using a *Edge Laplacian 5x5* filter: the test 640 kg shot (bottom left, see also Figure 1) and the main explosion (bottom right).

Speed Video Records

The speed camera Phantom v5.1 was placed at ~750 m; the actual frame rate was 3902 fps. Sample snapshots are presented in Figure 4. The Cine Viewer 675 software was used for processing and visual analysis of raw data.

Unfavorable lighting conditions prevented aerial observation of the shock wave. As for the test shot (Figure 4), it was revealed only on the ground, close to the camera, at ~1.5 seconds after the detonation. Observed anomalous nonuniform expanding of the fireball and detonation products indicates possible nonlinear directivity effects.

Observation of the Explosion Crater

Initial coarse estimations by measuring tape showed a crater radius of R ~13.5 m (Figure 5). The Survey of Israel team conducted accurate GPS crater measurements just after the explosion and provided appropriate crater 2D and 3D images, confirming the radius value and a depth estimation of H ~5 m (Figure 5).

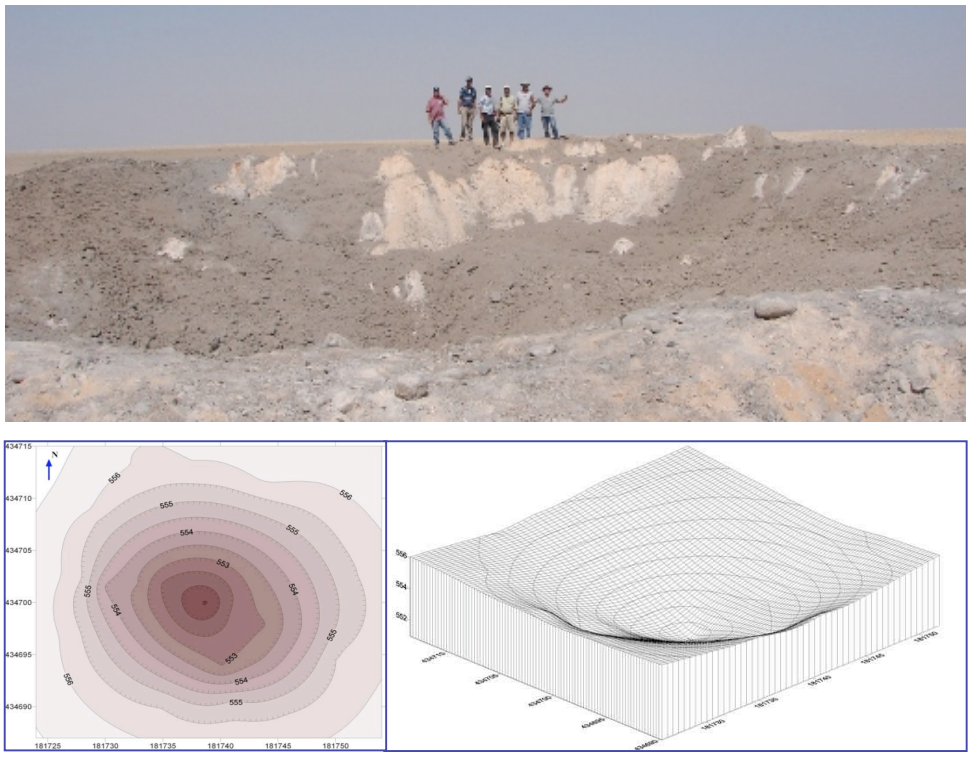

Figure 5. Crater created by the calibration explosion (top); 2D and 3D images provided by the Survey of Israel (bottom).

A similar hemispherical surface explosion of 90.7 tons of TNT, on alluvium, in the US Army Waterways Experiment (1962) created a much larger crater with R = 21.3 m, H =6 .3 m (CraterDatabase, 2004). For comparison, we also used empirical equations for craters of large-scale explosions on soft soil (Adushkin and Khristoforov, 2004):

$$R = 3.36W^{0.336}; \quad H = 1.78W^{0.316}, \tag{1}$$

where W is TNT equivalent yield, in tons.

According to Eq.(1), the measured radius 13.5 m fits to a charge of 63 ton, and the depth 5 m fits ~30 tons, whereas a charge of 82 tons should provide R ~15 m, H ~7 m. Thus the created crater was smaller than expected for this on-surface charge, according to similar explosions, indicating decreased coupling of explosive energy to the ground, supposedly due to the specific charge design and especially the upward detonation.

Accelerometer Measurements

Three K2 accelerometers of Kinemetrics were deployed prior to the explosion; Acc1 and Acc3 were co-located with pressure gauges (Figures 3, 6). The accelerometers were placed on the surface and were subjected to the impact of the strong air-shock wave on the sensor. Vertical acceleration of more than 4 g was measured at the closest Acc1, corresponding to the first shock; weaker secondary shocks were also found (Figure 7).

High-Pressure Measurements

High-pressure measurements were intended to evaluate energy generation for the new IMI explosives and the elaborated charge design and to provide a TNT yield estimation of the explosion. Six pressure gauges XTL-190-5G/50A/100A were installed in a line in the distance range of 100–600 m; the recording system (with a sampling rate of 2 MHz) was deployed in the half-buried concrete bunker at ~300 m (Figure 3).

Shock waves for the new explosives were expected to be weaker than for TNT, but all pressure gauges measured significantly larger free-field side-on peak pressure and positive phase impulse and more speed propagation, compared with predictions for the equal TNT charge (Figures 7–8). The closest sensor G1 was knocked down, and the unreliable record was excluded from the analysis (Figure 6).

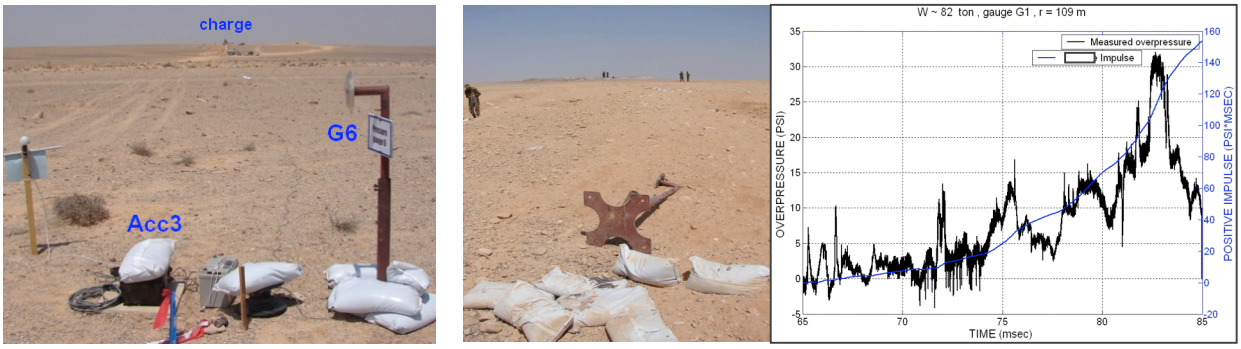

Figure 6. The most remote co-located accelerometer Acc3 and pressure gauge G6 at 611 m (left). The closest gauge G1 at 109 m after the explosion (center) and the record (right)

For all pressure gauges, a distinct secondary shock (SS) wave was observed during the negative phase portion of the pressure-time curves (Figure 7), showing positive peak amplitudes, as opposed to the case of surface ANFO shots 20 and 100 tons in Alberta, Canada, where all SS peak amplitudes were negative (Swisdak and Sadwin, 1970).

This SS phase clearly also occurred at all accelerograms, with appropriate time delay (Figure 7). We estimated from the records basic parameters of the air-blast wave: Time of Arrival T_A, Peak Pressure P_m, Positive Phase Impulse I_+, Positive Phase Duration τ_+, and (T_A, P_m) for the Secondary Shock. Due to some irregularities in the high-pressure time history, it was approximated by 2- or 3-exponent fit curves, for more reliable estimation of P_m and τ_+ values.

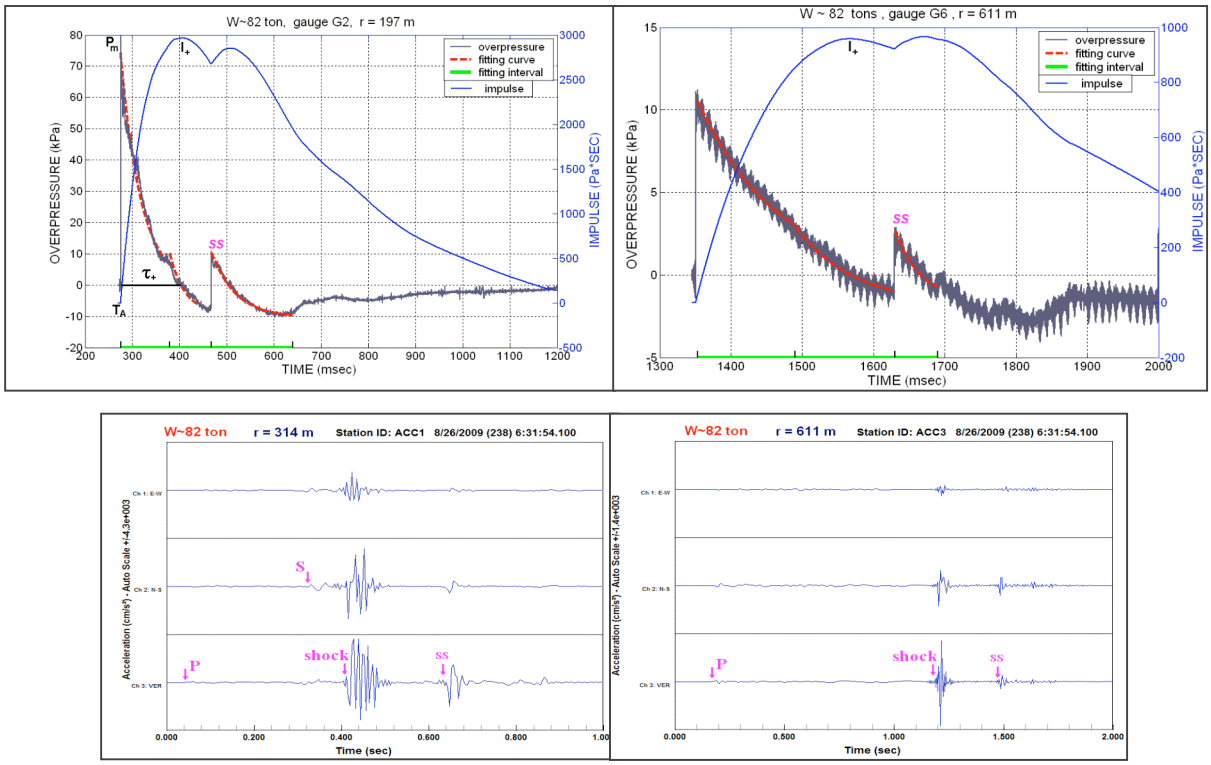

Figure 7. Sample records at two pressure gauges (top) co-located with accelerometers (bottom).

We used the DDESB Blast Effects Computer Version 4.0 (BECV4), an Excel template (Swisdak, 2000), for predicting the Sayarim air-blast parameters for the equal weight TNT charge of W = 81, 664 kg, actual altitude H = 556 m, and T = 35°C. Figure 8 shows a comparison of measured parameters P_m, τ_+, I_+, and T_A and the predicted values at different distances, where all parameters are evidence that the actual TNT equivalent yield was larger than the nominal charge weight. Comparison of measured P_m and T_A for the main and secondary shocks is also presented, where P_m for SS was calculated as the difference (the jump) between fit maximal and minimal amplitudes on the arrival time.

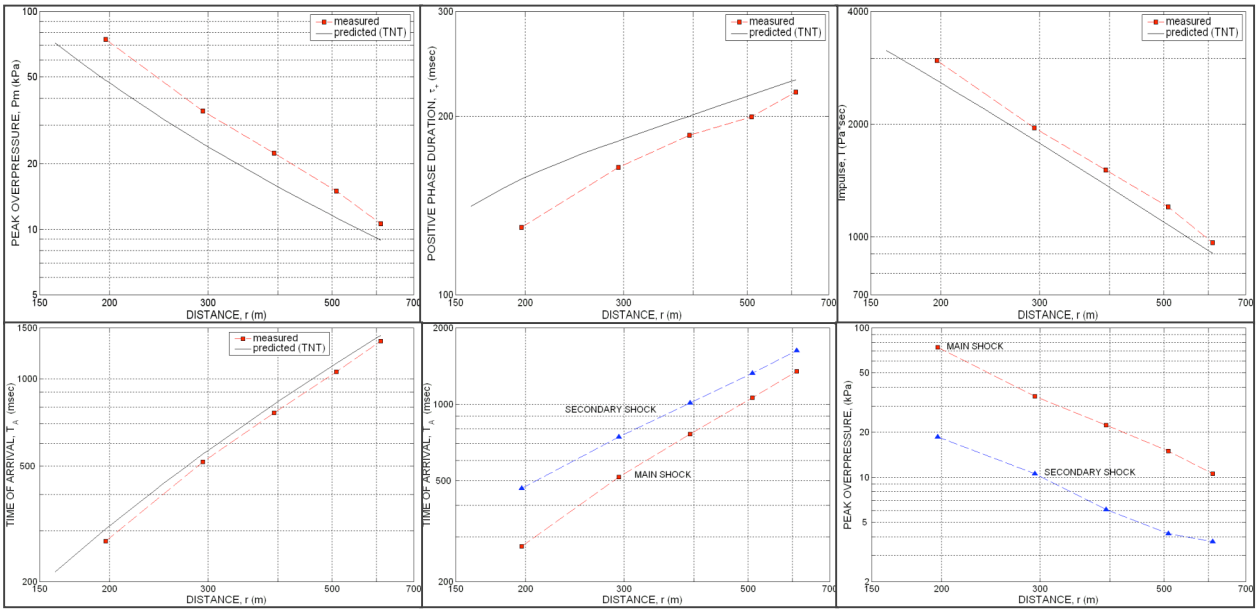

Figure 8. Comparison of measured free-field air-blast parameters with values predicted by BECV4 procedure for the surface explosion of 81,664 kg of TNT (H = 556 m, T = 35°C). Comparison of measured parameters for the main and secondary shocks is also shown.

Estimations of Equivalent TNT Yield

Estimations of equivalent TNT yield were obtained, using BECV4 procedure (Swisdak, 2000), for altitude 556 m, T = 35°C, based on measured airbast values, averaged over 5 gauges (Table 2). Increased P_m and decreased τ_+ values (Figure 8) resulted in appropriately overestimated and underestimated yields. The positive phase impulse I_+ is the integral and stable characteristic of the air-blast wave (unlike the one-point peak amplitude), and we consider the impulse-based estimation of 96 tons (~0.1 kt) as the most reliable. Note that it is close to the average of estimations by both parameters (P_m and τ_+) because the impulse is about proportional to their multiplication.

Table 2. Estimation of the TNT equivalent yield based on air-blast measurements (H = 556 m, T = 35°C).

Gauge	Distance, m	Peak Over-Pressure P_m		Positive Phase Duration τ_+		Positive Phase Impulse I_+	
		Measured, kPa	Yield, tons	Measured, msec	Yield, tons	Measured, Pa*sec	Yield, tons
G2	197	74.4	164	129.9	33	2963	101
G3	294	34.9	157	163.9	52	1953	93
G4	394	22.3	163	185.6	59	1508	95
G5	509	15.0	155	199.6	57	1202	98
G6	611	10.6	123	219.5	67	966	92
AVERAGE			**152**	**54**		**96**	

The obtained yield estimation is about 20% more than the nominal weight of the charge; we assume several possible factors of enhanced air-blast energy and the appropriate enlarged TNT yield: (1) high concentration of explosives, with minimal air voids between the charge units; (2) a very strong booster and multiple initiation scheme; (3) upward detonation of the charge; and (4) high detonation velocity (~10% higher than TNT).

Observations at Local Distances.

Seismic and acoustic signals were recorded at numerous permanent and portable stations in Israel, installed by GII. We also used data from an infrasound array deployed at Mt. Meron (IMA) by Israel NDC and an array at Cyprus (CYPR) and a close station UMUF, deployed by the Universities of Mississippi and Alaska (Fairbanks) (Figure 9). Seismic signals were recorded at ISN stations at 15–340 km, and strong acoustic phases (T) were observed at several close stations (up to 70 km) (Figure 9). At some stations amplitudes of acoustic phases were higher than the amplitudes of seismic signals. The estimated local (duration) magnitude of 2.5 was smaller than expected (~2.7–2.8)

for this on-surface charge; old ammunition shots with downward detonation showed maximal vertical amplitudes in P-waves, whereas for the calibration explosion with upward detonation, P-waves are much smaller than surface waves (Figure 9)—two more indications of a decreased impact on the ground due to the enhanced explosives energy coupling to the atmosphere.

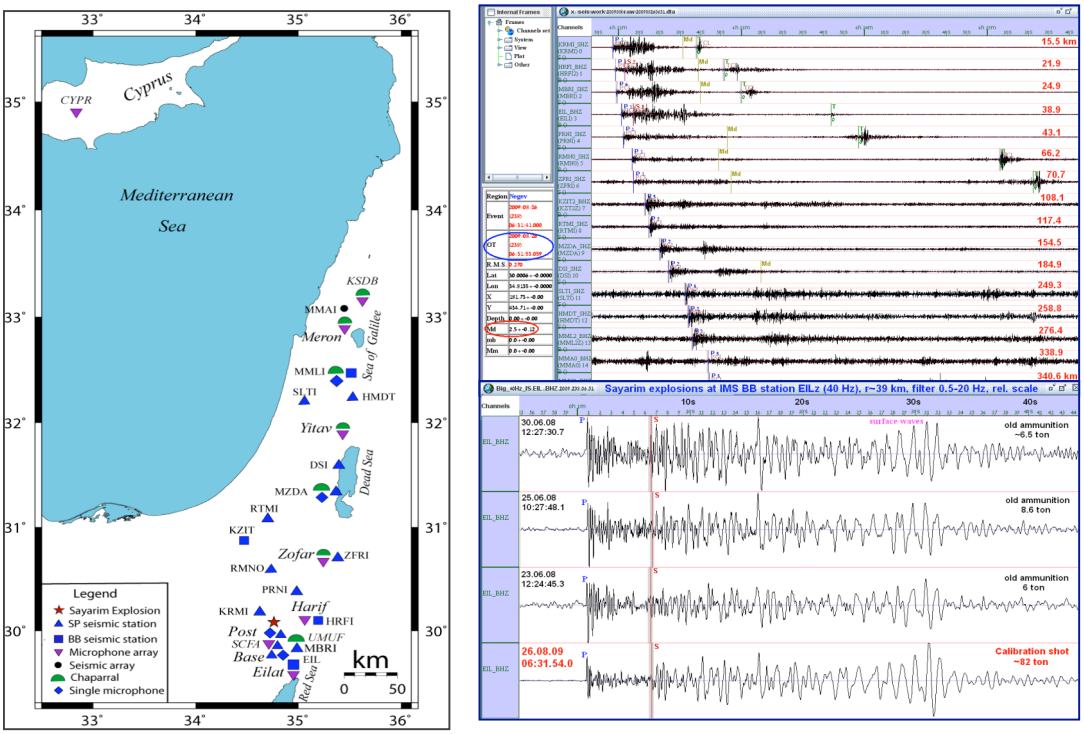

Figure 9. Map of recording stations used (left); seismic and acoustic phases (T) at ISN stations (top right); comparison of seismic waves (in relative scale) at IMS BB station EILz from three old ammunition shots (see Gitterman and Hofstetter, 2008) with the main explosion (bottom right).

Dominant Periods, Filtering Raw Records, and Yield Estimation

An empirical relationship between the yield Y_0 (tons) and the dominant period of the infrasound signal T_0 (sec) was derived by the U.S. Air Force Technical Applications Center from nuclear explosions above ground at the Nevada Test Site (ReVelle et al., 1998):

$$Y_0 = (2)\times 2.63\times T_0^{3.34} \quad , \tag{2}$$

where T_0 is the period at the signal maximal amplitude, and the doubling factor in brackets compensates for the nonnuclear nature of the explosions. The physical basis for this relation is found in the increased acoustic transit time of the blast radius with increased yield. The period is not influenced much by propagation like peak amplitudes. According to Eq. (2), for charges ~100 tons the dominant period should be T_0~2.4 sec, or f_0~0.4 Hz. Then, the high-pass filter frequency should be much lower, such as 0.1 Hz, in order not to cut the signal energy and distort waveforms.

When processing records of the Sayarim Calibration Explosion, filters 0.3–6 Hz for local Israel stations and 0.3–4 Hz for the far-regional I48TN station were used (O'Brien et al., 2010). Empirical yield-range-amplitude attenuation laws use the peak-to-peak amplitude (Pa) of the dominant stratospheric return at IMS stations, filtered from 0.5 to 3.0 Hz (Brown et al., 2009a). Table 3 shows that for these filter bands the energy and peak amplitude of infrasound signal was reduced notably, compared with the filter band 0.1–5 Hz, which we used when measuring dominant periods and peak pressure amplitudes of the signals.

Table 3. Peak amplitudes at Cyprus infrasound station (array) for different band-pass filtering

Sensor	Peak amplitude, units		Peak amplitude reduction, %	Peak amplitude, counts	Peak amplitude reduction, %
	Filter 0.1-5Hz	Filter 0.3-4Hz		Filter 0.5-3Hz	
CYPR1	13905	10447	25	8818	37
CYPR2	19258	13968	27	9108	53
CYPR3	65386	57940	11.4	43641	33

For the yield estimation, we utilized a dataset of Israel and Cyprus infrasound stations a range of 150–570 km, where single, clear main arrivals were observed. Dominant periods of the signals were accurately determined, using zero crossings; in some cases sinusoidal extrapolations were used to find the crossing of a signal curve with the zero level (Figure 10, Table 4). Yield estimation based on the average of dominant periods of infrasound signals is obtained: 128 tons of TNT. This value is also higher than the nominal charge weight of 82 tons and is relatively close to the estimated yield of ~0.1 kt, based on air-blast measurements.

Table 4. Measured dominant periods for the main explosion and the yield estimation

Station	Sensor type	Distance, km	Dominant period, sec
MZDB	Chaparral25	154	2.52
MMLB	Chaparral25	276	3.0
IMA1-5	MB2000	338	2.50,2.57,2.53, 2.50, 2.48
Meron_GII	Chaparral25	340	2.53
CYPR1-3	UM sensors	576	2.56,2.71,2.66
Average period T_0			**2.60**
standard deviation σ			0.106
Y_0 in formula (2)			**128 tons**

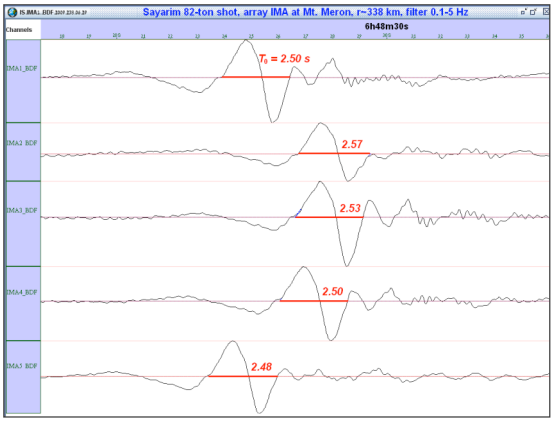

Figure 10. Sample of measuring the dominant period at IMA array.

Analysis of the Peak Amplitudes for Israel Stations

The most common empirical amplitude-yield scaling relation is based on data from a series of large-scale explosive tests at White Sands Missile Range (WSMR) during 1981–1993 with the charge range of 24–4880 tons of ANFO, recorded at distance range of 250–5300 km, with addition of the Watusi explosion (Whitaker et al., 2003), referenced also as LANL2003:

$$P = 5945.7\times(SR)^{-1.4072} \qquad SR = R/(2*W)^{0.5}, \tag{3}$$

where P is peak-to-peak, wind-corrected amplitude in Pa and SR is scaled range, W is yield in kilotons, and R is range in kilometers. The empirical wind-correction factor is given by $10^{-0.019v}$, where v is wind-component at 50 km altitude in m/s.

The peak amplitudes for the main explosion were measured at well-calibrated stations that recorded good-quality signals and wind-corrected using along-path wind v = 15 m/s, based on G2S specifications (O'Brien et al., 2010) and local radiosonde data. The signal at the close UMUF station was very strong and therefore clipped, and the peak value was extrapolated. The group velocity of the maximal (first) arrival at selected stations was ~340 m/s (except for UMUF ~350 m/s). Scaled range is calculated for W = 0.1 kt. The results are presented in Table 5 and Figure 11, demonstrating 3–5 times higher amplitudes, compared with the LANL2003 curve, thus indicating a possible upward directivity effect and asymmetric energy radiation to the atmosphere, appeared at these local distances. Using a

different new measure of the source-receiver wind showed that wind-corrected amplitudes for the main SMR shot (with W = 82 tons) agree closely with the LANL2003 relation at far-regional stations (O'Brien et al., 2010).

Table 5. Measured wind-corrected amplitudes at Israel stations (W = 0.1kT, v = 15 m/s, filter 0.1–5 Hz)

Station	Range R, km	Scaled range SR, km/kT$^{1/2}$	Peak-to-peak measured amplitude, Pa	
			raw	wind-corrected
UMUF	22.5	50.3	~280	~145
Zofar	72	161	23.5	12.19
MZDB	154	344	15.3	7.94
MMLB	276	617	7.48	3.88
IMA(aver)	338	756	3.93	2.04
Meron	340	760	4.23	2.19

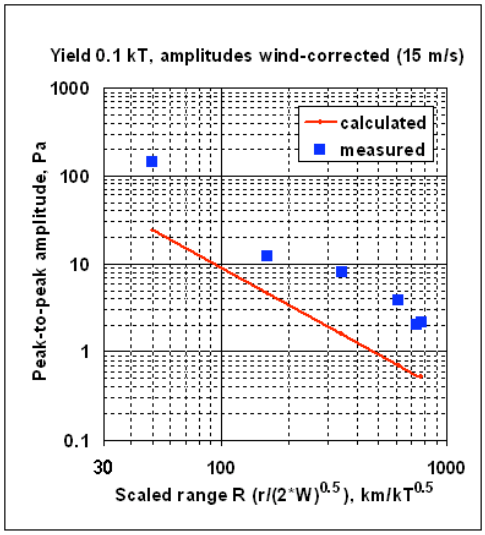

Figure 11. Measured wind-corrected amplitudes at Israel stations for the main SMR shot, compared with the LANL2003 curve (red).

Other Yield Estimations

An overestimated yield of 0.3–0.5 kT was obtained at IDC, using wind-corrected amplitudes at two far-regional IMS stations I26DE and I48TN, applied to several yield-range-amplitude attenuation laws, including LANL2003 (Brown et al., 2009b). Using a new-developed parabolic-equation-based semi-empirical relation, a reasonable value of ~0.1 kt at the dominant frequency was estimated from IS48 data (Le Pichon et al., 2010).

CONCLUSIONS AND RECOMMENDATIONS

A charge of about 82 tons of HE explosives, assembled as a special design pyramid on a soft sediment surface, was successfully detonated. Enhanced peak pressures at all distances and smaller crater and seismic magnitude confirmed that the developed charge design provided a strong explosion energy generation and necessary partition: more energy to the atmosphere and less to the ground. The estimated yield of 0.1 kt, based on the measured positive phase impulse in air-blast waves at near-source distances, can be considered as Ground Truth parameter.

The main goal of the Sayarim Calibration Experiment was reached: infrasound signals were observed at numerous stations at distances up to 3500 km (much more than planned) (Garces et al., 2009, Bowman et al., 2009), thus establishing the first Ground Truth GT0 infrasound dataset for Middle East/Mediterranean/ Europe region.
More similar explosions are necessary, in different seasons, to provide more data and some statistics, for refining and tuning IDC evaluation procedures of infrasound monitoring (especially yield estimation).

ACKNOWLEDGEMENTS

The Experiment Division of Israel Defense Forces provided the territory and valuable technical and logistic support (in preparation for the explosion), speed video recording, and high-pressure measurements. Private companies supplied effective HE explosives (IMI Ltd.) and prepared and assembled the charge (Elita Security Ltd.). The Israel NDC provided infrasound array observations at Mt. Meron. The Universities of Mississippi and Alaska (Fairbanks) installed the close station UMUF and the array at Cyprus. The Survey of Israel provided accurate crater measurements. The GII personnel conducted local measurements (U. Peled) and provided all necessary organizational support (R. Hofstetter) and the processing and graphic presentation of air-blast data (N. Perelman).

REFERENCES

Adushkin, V. V. and B. D. Khristoforov (2004). Craters of large-scale surface explosions, *Combust, Explo. Shock Waves* 40: 674–678.

Bowman, J. R., H. Israelsson, G. Shields, M. O'Brien, and Y. Gitterman (2009). Detection and characterization of infrasound signals at IMS stations from explosions at the Sayarim Military Range, Israel: 2005–2009, Infrasound Technology Workshop, Brasilia, Brazil, November 2–6, 2009.

Brown, D., I. Kitov, N. Brachet, P. Mialle, and R. Le Bras (2009). Enhancements to the CTBTO infrasound processing system, Infrasound Technology Workshop, Brasilia, Brazil, November 2–6, 2009.

CraterDatabase_V1.3, (2004). http://keith.aa.washington.edu/craterdata/

Garces M., D. Fee, R. Waxler, C. Hetzer, J. Assink, D. Drob, A. Le Pichon, Y. Gitterman, and R. Hofstetter (2009). The Sayarim Calibration Experiment: Theory and observations, Infrasound Technology Workshop, Brasilia, Brazil, November 2–6, 2009.

Gitterman, Y. and R. Hofstetter (2008). Infrasound Calibration Experiment in Israel: preparation and test shots, in *Proceedings of the 30th Monitoring Research Review: Ground-Based Nuclear Explosion Monitoring Technologies*, LA-UR-08-05261, Vol. 2, pp. 872–881.

Le Pichon A., J. Vergoz, L. Ceranna, D. Brown, G. Aubert, P. Mialle, and N. Brachet (2010). Towards an enhanced picture of the detection capability of the IMS infrasound network, EGU General Assembly 2010.

O'Brien M. S., J. R. Bowman, and G. Shields (2010). Infrasound signals from explosions at the Sayarim Military Range, Israel: 2005–2009, *Report SAIC-10/3001*.

ReVelle, D., R. Whitaker, and W. Armstrong (1998). Infrasound from the El Paso super-bolide of October 9, 1997, Los Alamos National Laboratory report LA-UR-98-2983.

Swisdak, M. and L. Sadwin (1970). Blast Characteristics of 20 and 100 ton hemispherical AN/FO charges, NOL data report, NOL TR 70-32, 17 Mar 1970.

Swisdak, M. (2000). DDESB Blast Effects Computer, Version 4.0.

Whitaker, R. W., T. D. Sandoval, and J. P. Mutschlechner (2003). Recent infrasound analysis, in *Proceedings of the 25th Seismic Research Symposium—Nuclear Explosion Monitoring: Building the Knowledge Base*, LA-UR-03-6029, Vol. 2, pp. 646–654.